Borrower: OCN

Lending String: *NHM,AFU,NOC,NOC,GZM

Patron: Tallmon, Sheila

Journal Title: Low temperature detectors LTD-13 Proceedings of the 13th International Workshop ; Stanford/SLAC, California, 20-24 July 2009 /

Volume: 1185 **Issue:**
Month/Year: December 16 2009 **Pages:** 450-453

Article Author: W. B. Doriese, et al;

Article Title: Optimal filtering, record length, and count rate in transition-edge-sensor microcalorimeters

Imprint: Melville, N.Y. ; American Institute of P

ILL Number: 68657186

Call #: online

Location: databases - AIP

ARIEL
Charge
Maxcost: 20IFM

Shipping Address:
ILL/Boulder Labs Library
U.S. Dept. of Commerce
325 BROADWAY - MC5
BOULDER, CO 80305-3328

Fax: boulderlabs.ill
Ariel: 140.172.211.165
Odyssey: 206.107.42.84

Optimal filtering, record length, and count rate in transition-edge-sensor microcalorimeters

W. B. Doriese*, J. S. Adams†, G. C. Hilton*, K. D. Irwin*, C. A. Kilbourne†, F. J. Schima* and J. N. Ullom*

*NIST, 325 Broadway, Boulder, CO 80305, USA
†NASA/Goddard Space Flight Center, Greenbelt, MD 20771, USA

Abstract. In typical algorithms for optimally filtering transition-edge-sensor-microcalorimeter pulses, the average value of a filtered pulse is set to zero. The achieved energy resolution of the detector then depends strongly on the chosen length of the pulse record. We report experimental confirmation of this effect. We derive expressions for the dependence of energy resolution on record length, and apply them to a pair of detector models for the X-ray Microcalorimeter Spectrometer instrument on NASA/ESA/JAXA's proposed International X-ray Observatory. Although the two models have identical pulse time-constants, they differ by a factor of two in the record length required to achieve a given energy resolution. Finally, we derive an expression for the maximum output count rate at high energy resolution of a TES pixel.

Keywords: count rate, International X-ray Observatory, microcalorimeter, optimal filter, spectrometer, transition-edge sensor
PACS: 95.55.Ka, 85.25.Oj, 07.85.Qe, 78.70.En

INTRODUCTION

As arrays of transition edge sensors (TESs) are developed for real-world applications, such as x-ray astronomy and synchrotron materials-analysis, instrument designers are examining the relationship between count rate and energy resolution. In this paper, we explore one aspect of this relationship: the dependence of energy resolution on the length of recorded pulse time-records.

Processing of TES pulses includes an optimal-pulse-height-estimation step[1], which has become known as "optimal filtering." The algorithm assumes that pulses of different energies differ in size but have the same shape, and employs a χ^2 minimization in which the frequency bins of the sampled pulse's discrete Fourier transform (DFT) are treated as independent measurements of the pulse height (a valid assumption in the case of stationary noise). Thus, the filter weights pulses by their signal-to-noise ratio (SNR) as a function of frequency.

The typical implementation[2] involves digitizing the detector time-stream into records of a fixed length, $t_{\rm rec}$. The signal portion of the filter is built as the DFT of the average of many triggered pulse records. The average of many spectra of pulse-free records makes up the noise portion. This implementation assumes that each pulse record contains only one pulse, so the chosen record length is intimately related to the achievable count rate.

A question has arisen recently[3] regarding how to treat the time average of the optimally filtered pulse, or alternatively, the f=0 bin of its DFT. This term contains an arbitrary and slowly varying offset, so most optimal-filter implementations discard it. However, the f=0 bin also contains true low-frequency signal and noise, and thus throwing it away reduces the SNR available for determining the pulse height. Since $t_{\rm rec}$ determines the size of the f=0 bin, the energy resolution of a TES depends on $t_{\rm rec}$. Interestingly, the TES decay-time constant is not necessarily a good predictor of what $t_{\rm rec}$ is necessary for a given energy resolution. Due to internal feedback mechanisms, two TESs can be designed with different internal time constants, but identical pulse rise- and decay-time constants. The internal time constants determine the importance of the discarded f=0 bin.

There are alternative schemes to the strict optimal filter to achieve higher count rates at the expense of some energy resolution. These include optimal filtering with a variable record length to avoid pulse pileup within records[4], and a trapezoidal filter that can process overlapping pulses[5]. Future optimal-filter implementations may also allow subtraction of the detector's quiescent signal-level at frequencies sufficiently low that the f=0 bin information may be at least partially recoverable, thus allowing shorter time records and higher count rates.

TES ENERGY RESOLUTION

In terms of its noise-equivalent power, the full-width-at-half-maximum energy resolution of a microcalorimeter with linear response and Gaussian, stationary noise sources is[6]:

$$\Delta E_{\rm FWHM} = \sqrt{8\ln 2}\left(\int_0^\infty \frac{4{\rm d}f}{{\rm NEP}^2(f)}\right)^{-1/2}. \qquad (1)$$

CP1185, *Low Temperature Detectors LTD 13, Proceedings of the 13th International Workshop*
edited by B. Cabrera, A. Miller, and B. Young
2009 American Institute of Physics 978-0-7354-0751-0/09/$25.00

Since TESs employ a SQUID-ammeter readout, Eq. 1 is more illuminating when expressed in TES-current units:

$$\Delta E_{\rm FWHM}/\sqrt{8\ln 2} = \tag{2}$$

$$\left(\int_0^\infty \frac{4\,|s_I(f)|^2\,{\rm d}f}{S_{I_{\rm TFN}}(f)+S_{I_{\rm J-TES}}(f)+S_{I_{\rm J-sh}}(f)+S_{I_{\rm amp}}(f)}\right)^{-1/2}.$$

Here, $s_I(f)$ is the power-to-current responsivity of the TES (and is also the FT of a current pulse divided by its photon energy). The various S_I terms are, referred to the TES current: the thermal-fluctuation (phonon), TES-Johnson, shunt-resistor Johnson, and amplifier (SQUID) noise spectra, and have units of A^2/Hz. From Eq. 2, we see that $\Delta E_{\rm FWHM}$ is determined by an integral over the squared signal-to-noise-ratio density (SNRD), which we write explicitly:

$$\Delta E_{\rm FWHM} = \sqrt{8\ln 2}\left(\int_0^\infty 4\ {\rm SNRD}^2(f){\rm d}f\right)^{-1/2}. \tag{3}$$

CONTRIBUTION OF THE f=0 TERM

The DFT of a data time-record of length $t_{\rm rec}$ has frequency bins of spacing ${\rm d}f = 1/t_{\rm rec}$. When the $\pm f$ terms of the DFT are combined to create a single-sided expression, the f=0 bin effectively contains information from $0 \le f \le {\rm d}f/2$. Discarding the lowest frequency bin thus turns $\int_0^\infty$ in Eqs. 1–3 into $\int_{1/(2t_{\rm rec})}^\infty$.

Fig. 1 demonstrates the importance of the f=0 bin. During a successful demonstration[7] of a prototype detector array for the proposed International X-ray Observatory's (IXO's) X-ray Microcalorimeter Spectrometer (XMS) instrument, in which 16 pixels from a GSFC detector array were read out through a 2-column × 8-row NIST time-division multiplexer with $\langle\Delta E_{\rm FWHM}\rangle$ = 2.9 eV at 6 keV, we recorded many hours of raw, multiplexed data in various configurations. We randomly chose a pixel from a recorded 2-column × 4-row raw data stream, and played back its data many times, each time selecting a different record length, while recording sets of triggered pulse and noise records. Figs. 1(a) and (b) show the measured average pulses and noise, and also pulses and noise from a numerical model of the pixel. Fig. 1(c) shows $\Delta E_{\rm FWHM}$ as a function of $t_{\rm rec}$. The dataset with the shortest records showed a whopping 0.5 eV of degradation in $\Delta E_{\rm FWHM}$.

THE EFFECTIVE FREQUENCY ($f_{\rm eff}$)

Since ${\rm SNRD}^2(f)$ (Eq. 3) typically approaches a constant value at low f, its rolloff can be thought of as having an

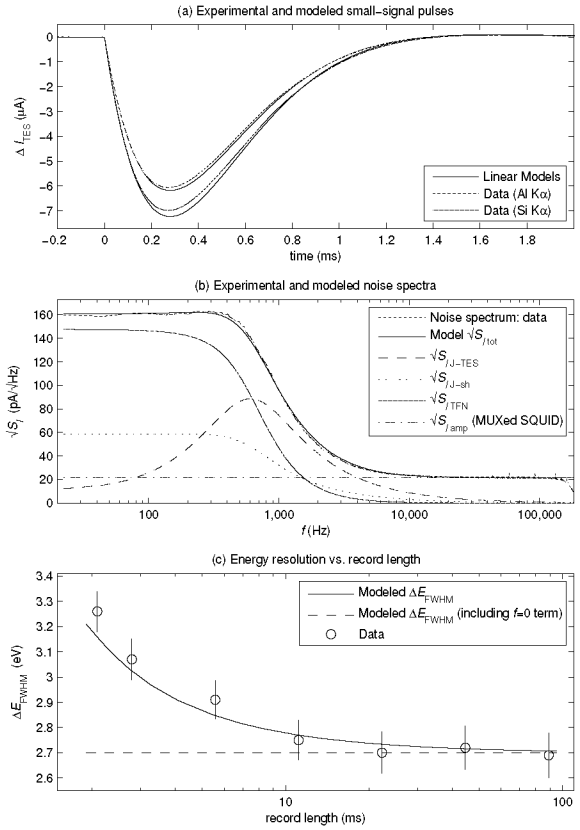

FIGURE 1. (a) Experimental (red, blue) and modeled (black) pulses from Al and Si Kα lines, (1.49 and 1.74 keV). The detector (C0R6 from our previous work[7]) was designed for 6 keV x-rays, so these low-energy lines are comfortably in the detector's linear regime. The critically damped time constant was $\tau_{\rm crit}$ = 280 μs. (b) Noise model and data. The four blue lines show the modeled noise components of Eq. 2. The black line is the total modeled noise; spectral data are shown in red. (c) Energy resolution vs. record length (logarithmic x-axis). The dashed line shows the prediction of Eq. 2's numerical integral, based on the modeled signal and noise from (a-b). The solid curve is the predicted energy resolution when the frequencies in the range $0 \le f \le {\rm d}f/2$ are not included in the integral. Open circles show the experimentally measured energy resolution as $t_{\rm rec}$ is varied from 2.1 to 89 ms (7.5 to 318 $\tau_{\rm crit}$). The input count rate from a cryogenic ^{55}Fe source was about 2.2 Hz. Analysis of the same raw data set of ~22,000 input pulse events with different $t_{\rm rec}$ allowed measurement of $\Delta E_{\rm FWHM}$ at the 5.9 keV Mn Kα complex with sub-0.1 eV 1-σ statistical error bars and no systematic drift among datasets.

"effective frequency,"

$$f_{\rm eff} = \frac{\int_0^\infty {\rm SNRD}^2(f){\rm d}f}{\lim_{f\to 0}{\rm SNRD}^2(f)}, \tag{4}$$

such that a low-frequency bin of width ${\rm d}f$ is one of a number, $f_{\rm eff}/{\rm d}f$, of independent SNR bins. Since the bins contribute to $\Delta E_{\rm FWHM}$ in quadrature, for ${\rm d}f \ll f_{\rm eff}$,

discarding the f=0 bin affects the energy resolution as

$$\Delta E\left(t_{\rm rec}\right) = \left(\lim_{t_{\rm rec}\to\infty} \Delta E\right)/\sqrt{1-1/\left(2t_{\rm rec}f_{\rm eff}\right)}. \quad (5)$$

Many authors have expressed Eq. 2 in terms of the parameters of a simple (single heat capacity, C; single thermal conductance, G) TES microcalorimeter in the linear (small-signal) limit; here we follow the formalism of Irwin and Hilton[8].

In general, Eq. 2's integral is not solvable in closed form, so $f_{\rm eff}$ is determined numerically from Eq. 4. However, when the amplifier-noise term is negligible, Eq. 2's integrand takes the form, $A_{\rm LP}^2/(1+(2\pi f\tau_{\rm LP})^2)$, which is the power response of a one-pole, low-pass filter with time constant $\tau_{\rm LP}$ and gain term $A_{\rm LP}$. The effective bandwidth of such a filter, via Eq. 4, is $f_{\rm eff} = 1/(4\tau_{\rm LP})$. In terms of TES model parameters, it is

$$f_{\rm eff} = \frac{1}{4\tau}\sqrt{\frac{T_{\rm c}R_0\xi + T_{\rm L}R_{\rm L}\left(\mathscr{L}_I-1\right)^2 + \frac{T_{\rm c}^2GF\left(T_{\rm c},T_{\rm b}\right)\mathscr{L}_I^2}{I_0^2}}{T_{\rm c}R_0\xi + T_{\rm L}R_{\rm L}}}. \quad (6)$$

Here, $\tau = G/C$ is the natural time constant; $T_{\rm c}$, $T_{\rm L}$, and $T_{\rm b}$ are the TES-operating, shunt-resistor, and bath temperatures; R_0 and $R_{\rm L}$ are the TES-operating and shunt resistances; I_0 is the operating current; $\mathscr{L}_I = (P_0\alpha_I)/(GT_{\rm c})$ is the constant-current loop gain; P_0 is quiescent bias power; $\alpha_I = \partial\log R/\partial\log T|_I$ is the (unitless) slope of the TES transition; $F\left(T_{\rm c},T_{\rm b}\right)$ contains the (unitless) physics of phonon exchange across G; and ξ is the (unitless) ratio of the total TES resistive noise to the equilibrium Johnson noise.

TWO MODELS FOR THE IXO XMS

Multiplexer (time-division, frequency-division, or code-division) bandwidth is used most efficiently under the condition of critical damping[8], in which the inductance, L, in the TES bias loop is chosen so the pulse rise- and decay-time constants have the same value, $\tau_{\rm crit}$. Multiplexing is easiest when $\tau_{\rm crit}$ is slowest. However, Eq. 5 shows that the record length is minimized (and count rate maximized) for a given $\Delta E_{\rm FWHM}$ when $f_{\rm eff}$ is maximized. Here, we develop two models to show that $\tau_{\rm crit}$ and $f_{\rm eff}$ can be adjusted at least somewhat independently. We use the property that changes in parameters such as $R_{\rm L}/R_0$, which affect primarily the TES's internal feedback mechanisms, change $\tau_{\rm crit}$ much more than they change $f_{\rm eff}$.

The baseline specification for the IXO XMS is a 32 × 32 array of multiplexed pixels that are similar to the ones we have previously demonstrated[7]. Multiplexed resolution should be $\Delta E_{\rm FWHM} \le 2.5$ eV up to $E_\gamma =$ 10 keV, and $\tau_{\rm crit}$ is tentatively specified to be 300 μs, although perhaps count rate is a better metric than $\tau_{\rm crit}$.

TABLE 1. Calculated parameters for the G=250 and 500 pW/K models. Symbols are defined in the text.

Param.	Derivation	G_{250} val.	G_{500} val.	units
P_0	$\frac{G(T_{\rm c}^n-T_{\rm b}^n)}{nT_{\rm c}^{n-1}}$	7.29	14.58	pW
I_0	$\sqrt{P_0/R_0}$	85.4	120.8	μA
$R_{\rm L}$	$\tau_{\rm crit}$=300 μs	638.3	956.1	$\mu\Omega$
L	crit. damping	243.0	187.4	nH
$f_{\rm eff}$	see Eq. 6	1.019	2.063	kHz
$\Delta E_{\rm FWHM}$	$S_{I_{\rm amp}} = 0$, $t_{\rm rec}\to\infty$	2.13	2.18	eV
$\sqrt{S_{I_{\rm amp}}}$	for MUXed $\Delta E_{\rm FWHM}$=2.4 eV as $t_{\rm rec}\to\infty$	36	21	$\frac{\rm pA}{\sqrt{\rm Hz}}$
$I_{\rm PH}$	Mn Kα_1 pulse height	27.5	50.4	μA

We develop two possible IXO detector models that both have $\tau_{\rm crit} = 300$ μs, but differ in $f_{\rm eff}$.

The following TES parameters are similar to those of the GSFC detectors from our previous IXO demonstration, and are common to the two models:

- $T_{\rm c} = 100$ mK
- $T_{\rm b} = 50$ mK
- $\alpha_I = 75$ (unitless)
- $\beta_I = \partial\log R/\partial\log I|_T = 1.25$ (unitless)
- $C = 1.00$ pJ/K
- $R_0 = 1$ mΩ
- $n = 3$ (thermal conductivity index, unitless).

The models diverge in their values of the thermal conductance: the "G_{250}" model has $G = 250$ pW/K, which is similar to the demonstrated value, while in the "G_{500}" model, G is increased to 500 pW/K to speed up the natural (no-feedback) response time, $\tau = C/G$. Shunt resistance is chosen in each case to achieve $\tau_{\rm crit} = 300$ μs, and then L is selected to enforce critical damping. For simplicity, we ignore that α_I and β_I will vary with I_0, and thus with G [9]. Table 1 contains the model details.

With respect to the standard G_{250} detector model, the G_{500} model, with twice the bias power and half the natural time constant, requires a larger shunt resistor to decrease electrothermal feedback and thus slow $\tau_{\rm crit}$ back to 300 μs. The larger shunt resistor also worsens the base energy resolution slightly, to 2.18 (vs. 2.13 eV). Interestingly, although the G_{500} model has a pulse height that is almost twice as high, it can tolerate far less amplifier (SQUID) noise before degrading to 2.4 eV. The goal of the exercise is achieved: the two models have the same value of $\tau_{\rm crit}$, but differ in $f_{\rm eff}$ by a factor of two.

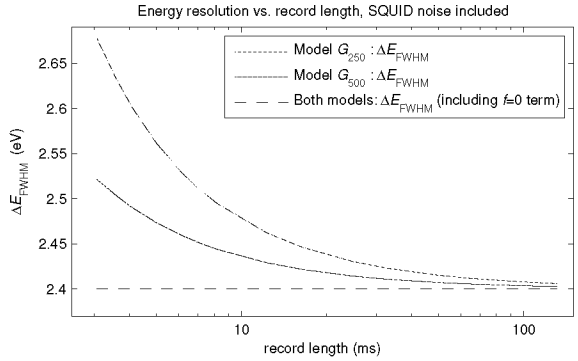

FIGURE 2. Energy resolution vs. record length for the standard (G_{250}, red) and high-G (G_{500}, blue) models, calculated from Eq. 2 with lower limit of integration $f = 1/(2t_{\rm rec})$. Both pulse models have the same critical time constant, $\tau_{\rm crit} = 300\ \mu$s. White SQUID amplifier noise has been included in each model such that $\Delta E_{\rm FWHM} = 2.4$ eV in the limit of long $t_{\rm rec}$ (see Table 1 for the values of $\sqrt{S_{I_{\rm amp}}}$). The G_{250} model requires $t_{\rm rec} > 7.8$ ms (26 $\tau_{\rm crit}$) to maintain IXO's $\Delta E_{\rm FWHM} < 2.5$ eV resolution specification, while the G_{500} model requires only $t_{\rm rec} > 3.8$ ms (13 $\tau_{\rm crit}$).

Fig. 2 shows how the energy resolution varies with record length for the two detector models. As expected, based on Eq. 5, $t_{\rm rec}$ can be half as long in the high-G model as in the standard-G model before the IXO resolution specification of 2.5 eV is reached. This increases by a factor of two the allowable count rate, while leaving the pulse shape the same for ease of multiplexing.

Although increasing G while maintaining $\tau_{\rm crit}$ decreases the needed $t_{\rm rec}$, this trick is clearly not a panacea. Higher-G pixels dump more bias power into the array. In addition, the rearrangement of the internal time constants and noise terms makes the G_{500} model more sensitive to amplifier noise, which can be a problem if the multiplexed readout is already amplifier-noise limited. Understanding of the TES's signal-to-noise frequency profile is simply one more trick in the detector designer's toolbox.

RECORD LENGTHS & COUNT RATES

Until now, our discussion has centered on $t_{\rm rec}$. Here we derive the maximum output count rate as a function of $t_{\rm rec}$, following the arguments of Knoll[10].

Photon events are Poisson distributed in time with average input count rate, n; r is the output count rate of events that can be filtered with the highest energy resolution. Such an event's arrival must meet two criteria: (1) another pulse cannot arrive within an interval $t_{\rm rec}$ afterward; (2) another pulse cannot have arrived within an interval $t_{\rm RTB}$ beforehand. The "return-to-baseline" time defines an interval such that a pulse doesn't sit on the tail of the previous one; its value is usually about 6–8 $\tau_{\rm crit}$. Perfect triggering of input events (equivalent to no triggering dead-time), a reasonable assumption given clever triggering algorithms[4] and $\tau_{\rm crit} \ll 1/n$, yields $r = ne^{-n(t_{\rm rec}+t_{\rm RTB})}$. The input rate $n = 1/(t_{\rm rec}+t_{\rm RTB})$ maximizes r with respect to n, so the maximum output rate of highest-resolution counts is $r_{\rm max} = 1/[(t_{\rm rec}+t_{\rm RTB})e]$.

The IXO G_{500} model requires $t_{\rm rec} > 3.8$ ms to keep $\Delta E_{\rm FWHM}$ from degrading past 2.5 eV (from its $t_{\rm rec} \rightarrow \infty$ value, which includes SQUID noise, of 2.4 eV; see Fig 2). We guess $t_{\rm RTB} = 7\tau_{\rm crit} = 2.1$ ms. The maximum output rate of high-resolution G_{500} counts is then $r_{\rm max} = 62$ Hz, and occurs at an input rate of $n = 169$ Hz. Via similar reasoning, a G_{250} pixel would have only $r_{\rm max} = 37$ Hz at an input rate of $n = 101$ Hz.

CONCLUSION

Our experiments and models show that discarding the f=0 bin when optimally filtering TES pulses causes the energy resolution to be a function of record length. Future development will explore the use of data before and after each record to fit and subtract the detector's quiescent signal level. If this can be done at sufficiently low frequencies and without contamination from pulse pileup, the f=0 bin information may be at least partially recoverable, which would allow shorter time records without an energy-resolution penalty.

This work was funded in part by NASA's ROSES program. Contribution of agencies of the United States government; not subject to copyright.

REFERENCES

1. S. H. Moseley, R. L. Kelley, R. J. Schoelkopf, A. E. Szymkowiak, D. McCammon, and J. Zhang, *IEEE Trans. Nucl. Sci.* **35**, 59–64 (1988).
2. A. E. Szymkowiak, R. L. Kelley, S. H. Moseley, and C. K. Stahle, *J. Low Temp. Phys.* **93**, 281–285 (1993).
3. Marcel van den Berg, *private communication* (2005).
4. R. L. Kelley, and 27 co-authors, *Pub. Astron. Soc. Jap.* **59**, 77–112 (2007).
5. H. Tan, et al., *these proceedings* (2009).
6. S. H. Moseley, J. C. Mather, and D. McCammon, *J. Appl. Phys.* **56**, 1257–1262 (1984).
7. C. A. Kilbourne, W. B. Doriese, and 14 co-authors, "Multiplexed readout of uniform arrays of TES x-ray microcalorimeters suitable for Constellation-X," in *SPIE Conference Series*, 2008, vol. 7011.
8. K. D. Irwin, and G. C. Hilton, "Transition-Edge Sensors," in *Cryogenic Particle Detection*, edited by C. Enss, Springer-Verlag, Berlin Heidelberg, 2005, vol. 99 of *Topics in Applied Physics*, pp. 63–149.
9. S. J. Smith, et al., *these proceedings* (2009).
10. G. F. Knoll, *Radiation Detection and Measurement*, John Wiley & Sons, Inc, New York, 2000, pp. 119–122, 636–642, 3rd edn.